applied sciences

MDPI

*Article*

# Physical and Mechanical Characteristics of Variotropic Concrete during Cyclic and Continuous Sulfate Attack

**Evgenii M. Shcherban' [1], Sergey A. Stel'makh [2], Alexey N. Beskopylny [3,*], Levon R. Mailyan [2], Besarion Meskhi [4], Diana Elshaeva [2] and Andrei Chernil'nik [2]**

[1] Department of Engineering Geology, Bases, and Foundations, Don State Technical University, 344003 Rostov-on-Don, Russia
[2] Department of Unique Buildings and Constructions Engineering, Don State Technical University, 344003 Rostov-on-Don, Russia
[3] Department of Transport Systems, Faculty of Roads and Transport Systems, Don State Technical University, 344003 Rostov-on-Don, Russia
[4] Department of Life Safety and Environmental Protection, Faculty of Life Safety and Environmental Engineering, Don State Technical University, 344003 Rostov-on-Don, Russia
* Correspondence: besk-an@yandex.ru; Tel.: +7-8632738454

**Abstract:** The concrete of numerous buildings and structures is at increased risk due to various kinds of aggressive pollutants. In this regard, it is necessary to implement and take additional actions, among which the so-called technological methods for concrete structure property modification are promising. These methods comprise improvement and modernization of existing technologies to produce the most effective concrete building structures before the introduction of steel reinforcement. One of the effective and proven technological and design solutions is the use of centrifuged and vibrocentrifuged concrete of an annular section with a variotropic concrete structure. The aim of the work was to study the physical and mechanical properties of variotropic concretes of annular structures when exposed to sulfate attack. As a result of the cyclic impact of sulfate attack, the mass loss of vibrocentrifuged concrete was the smallest in comparison with centrifuged (17% less) and vibrated concrete (37% less). The loss of cube and prism strength of vibrocentrifuged concrete was the smallest in comparison with centrifuged (20% and 18% less, respectively) and vibrated concrete (42% and 38% less, respectively). The sulfate attack rate, as a depth of penetration and concrete destruction, was 46% less for vibrocentrifuged concrete than for centrifuged concrete and 65% less than for vibrated concrete.

**Keywords:** concrete sulfate attack; variotropic concrete; vibrocentrifuged concrete

check for updates

**Citation:** Shcherban', E.M.; Stel'makh, S.A.; Beskopylny, A.N.; Mailyan, L.R.; Meskhi, B.; Elshaeva, D.; Chernil'nik, A. Physical and Mechanical Characteristics of Variotropic Concrete during Cyclic and Continuous Sulfate Attack. *Appl. Sci.* **2023**, *13*, 4386. https://doi.org/10.3390/app13074386

Academic Editors: Cesare Oliviero Rossi and Dario De Domenico

Received: 16 February 2023
Revised: 22 March 2023
Accepted: 29 March 2023
Published: 30 March 2023



## 1. Introduction

### *1.1. Background*

Currently, construction around the world is growing significantly due to an increase in the pace and volume of construction work. Structures are being built around the world, including multi-story buildings and houses with numerous large rooms, and reinforced concrete remains the primary building material for such buildings. While reinforced concrete, of course, has a number of advantages, it has several risks associated with the problems of ensuring its reliability and one of the main stages of durability. Undoubtedly, one of the main risks of reinforced concrete structures in terms of durability is their corrosion resistance. The fact is that a large number of operated structures of buildings and structures are at increased risk because of various kinds of corrosive effects on these buildings and structures. In this regard, it is necessary to implement and take additional measures for such buildings and structures to protect them from corrosion factors and corrosive effects. There are several methods for protecting against corrosion effects—these can be methods based on the composition of concrete mixtures, that is, prescription, and methods based on creating an additional protective layer and deepening the reinforcement into the concrete body, that is, constructive [1]. However, in our opinion, the so-called technological methods are promising: these are the improvement and modernization of existing technologies for the production of the most effective structures made of concrete in order to protect the concrete structure from corrosion.

The problem of research from a practical point of view is the premature failure of reinforced concrete structures. From a scientific point of view, the problem is the scientific lack of a systematic base of fundamental and applied knowledge about the relationship between the composition, manufacturing technology, structure, and properties of concrete under sulfate attack conditions. In [2–6], the authors studied the effect of sulfate attack on the physical and mechanical characteristics of various types of concrete. In [2], it was found that the best values of the coefficient of corrosion resistance were recorded for self-compacting concrete with a fly ash content of 40% [2]. The effective use of fly ash for the manufacture of high-performance self-compacting concrete with increased resistance to sulfates is also confirmed in [3]. In [4], the authors considered two different modes of sulfate attack, namely full immersion, simulating the chemical impact of sulfate, and cyclic exposure, in which laboratory samples with fly ash and metakaolin showed the highest resistance. Partial replacement of cement with incinerated municipal solid waste and bottom ash improves the performance of concrete against sulfate attack, namely reducing capillary porosity and increasing durability [5]. In addition, the degradation of concrete structures can be reduced by using modified concrete containing sulfur, fly ash, microsilica, and nanoparticles such as silicon dioxide [6].

The relationship between the penetration of chloride ions and the specific resistance of concrete modified with the addition of two types of calcined ore, namely raw and calcined, was considered in [7]. According to the research results, concrete with the addition of calcined raw ore has the highest resistance and the lowest diffusion coefficient of chlorides in comparison with ordinary concrete, and concrete with the addition of calcined ore. In [8], an assessment was made of the effect of acid corrosion on the mechanical properties of concretes subjected to monotonous and cyclic loads. According to the results of the study, it was found that acid corrosion proceeds more intensively under cyclic loads. The surface of corroded concrete cracked more easily and collapsed under the load. In addition, with an increase in the duration of the aggressive impact, the deformation of concrete increases. An assessment of the influence of various modifying substances on the increase in the resistance of concrete to corrosion is presented in [9,10]. The addition of copolymers makes it possible to increase the resistance of concrete to corrosion, which is confirmed by the studies presented in [11]. In addition, there are a huge number of ways to increase corrosion resistance by using modifying additives (limestone powder [12], quartz [13], slag [14], limestone and metakaolin [15]), various types of cement [16,17], basalt fiber [18,19], waste rubber from tires for partial replacement of natural filler [20], and polymer additives [21]. The influence of prescription factors on the corrosion resistance of solutions was studied in [22,23]. In this case, $Ca^{2+}$ [22] and magnesium potassium phosphate cement [23] depending on the age of hydration were considered as influencing factors. The resistance of concrete to corrosion is affected by the level of concentration of aqueous solutions of chloride and sulfate media [24], as well as already existing structural defects in the form of cracks [25]. At the same time, attention was paid to the mechanisms of damage and degradation of concrete, as well as the diffusion of chloride ions.

The effect of sulfate attack has also been evaluated on the properties and behavior of concrete products such as square steel tube columns filled with concrete [26] and twisted piles [27]. Considering reinforced concrete as a whole, in addition to concrete corrosion, it is necessary to touch upon the corrosion of reinforcing steel, which also has a negative impact on the operation of products and structures. In this area, many materials and methods have already been considered to protect reinforcing steel from various types of corrosion [28–31].

The practical consequences of corrosion of reinforced concrete structures in terms of greater seismic vulnerability, lower bearing capacity, and alteration of the failure mechanism (from ductile to more brittle) are considered in [32,33]. The seismic resistance margin of supporting structures located near the sea decreased to 20–40%, while the weight loss of steel reinforcing bars was 20–30% [32]. The main parameters (degree of corrosion and adhesion behavior at the steel–concrete interface) that affect the safety of corroded reinforced concrete structures (mechanical properties and failure mechanism) play an important role in determining failure modes under various corrosion scenarios [33].

### *1.2. Rationale*

All studied works are mainly focused on prescription methods for increasing the resistance of concrete to corrosion, as well as products and structures made of them. The analysis of the literature revealed a lack of work related to technological methods for increasing the resistance of concrete to corrosion. At the same time, it is known from the previously published works of our team and other authors [34–43] that one of the effective and proven technological and design solutions is the use of centrifuged and vibrocentrifuged reinforced concrete structures of an annular section with a variotropic concrete structure. Under the variotropic structure of concrete, such a structure of concrete of the annular section of a reinforced concrete element, which has characteristics that differ in the diameter of the section, is understood. At the same time, the inner layer has the lowest characteristics, the middle layer has higher characteristics, and, finally, the outer layer has the best characteristics and, in turn, is designed to protect the structure from various kinds of degradation effects.

Thus, the scientific novelty of the study will be the first created data system for three technologies: vibrating, centrifuging, and vibrocentrifuging of concrete, depending on sulfate attack. That is, the difference from the past will be the first studied resistance of variotropic concrete to sulfate attack and the experimental and analytical comparison with the resistance to sulfate attack of traditional vibrated concrete. The aim of the work is to study the physical and mechanical properties of variotropic concretes of annular structures when exposed to sulfate attack, to analyze the advantages of such a technological approach, and to identify differences in properties between concretes made using different technologies and having different structures when exposed to sulfate attack. The objectives of the study is to develop a system of methods and approaches to justify the technological and structural advantages of variotropic concretes over conventional ones; study the issues of concrete sulfate attack; conduct our own experimental research on three technologies: vibrating, centrifuging, and vibrocentrifuging of concrete; obtain results and their analytical processing with subsequent discussion to formulate new theoretical knowledge; and develop practical applied proposals for the real construction industry on issues related to concrete elements of buildings and structures under sulfate attack conditions.

## 2. Materials and Methods

### *2.1. Materials*

Sulfate-resistant Portland cement (SRPC) grade CEM II/A-Sl 42.5 N SR (Starotsementny plant, Sukhoi Log, Russia) was used to produce concrete mixtures. This cement has the following characteristics of Portland cement clinker:

- The content of $C_3A$ is 2.95%;
- The content of $C_3A + C_4AF$ is 20.3%.

The chemical composition of sulfate-resistant Portland cement is presented in Table 1.

**Table 1.** Chemical composition of SRPC.

| Grade of Cement | $SiO_2$ (%) | $Al_2O_3$ (%) | $Fe_2O_3$ (%) | CaO (%) | MgO (%) | $SO_3$ (%) | $Cl^-$ (%) | Alkali Oxides, % |
|---|---|---|---|---|---|---|---|---|
| CEM II/A-Sl 42.5 N SR | 21.29 | 4.46 | 5.12 | 64.48 | 1.63 | 2.56 | 0.02 | 0.44 |

The physical characteristics of SRPC have the following meanings (Table 2).

**Table 2.** Physical characteristics of SRPC.

| Blaine Specific Surface Area ($m^2$/kg) | Start/End Setting (h:min) | Normal Density (%) | Uniformity of Volume Change (mm) | Compressive Strength after 28 Days (MPa) |
|---|---|---|---|---|
| 284 | 2:40/3:45 | 24 | 3 | 49.7 |

As a coarse and fine aggregate, crushed stone from sandstone of a fraction of 5–10 mm from the Obukhovskoye deposit (Fedorovsky rubble plant, Shakhty, Russia) and quartz sand from the Astakhovsky quarry (Quartz, Shakhty, Russia) were used. The physical and mechanical characteristics of crushed stone are presented in Table 3, and those of sand are presented in Table 4.

**Table 3.** Characteristics of coarse aggregate.

| Crushability Grade | The Content of Lamellar and Needle-Shaped Grains (%) | The Content of Dust and Clay Particles (%) | Bulk Density (kg/$m^3$) | Density (kg/$m^3$) | Void Ratio (%) | Content of Grains of Weak Rocks (%) | Frost Resistance (Number of Cycles) |
|---|---|---|---|---|---|---|---|
| 1000 (weight loss from 11% to 13% according to GOST 8269.0 [44]) | 6.9 | 0.3 | 1432 | 2640 | 44 | 1.4 | 200 |

**Table 4.** Characteristics of fine aggregate.

| Grain Composition | | | | | | | Size Modulus | The Content of Dust and Clay Particles (%) | Bulk Density (kg/$m^3$) | Density (kg/$m^3$) |
|---|---|---|---|---|---|---|---|---|---|---|
| Sieve Size (mm) | | | | | | | | | | |
| Retained (%) | | Retained and Cumulative Retained (%) | | | | | | | | |
| 10 | 5 | 2.5 | 1.25 | 0.63 | 0.315 | 0.16 | 1.63 (small according to GOST 8735-88 [45]) | 0.87 | 1496 | 2605 |
| 0 | 0 | 0.15 | 1.39 | 8.16 | 44.87 | 42.73 | | | | |
| | | 0.15 | 1.54 | 9.70 | 54.57 | 97.30 | | | | |

Solutions for modeling an aggressive environment were prepared by dissolving $Na_2SO_4$ (Pentan, Krasnodar, Russia) and $H_2SO_4$ sulfuric acid (Evrokhim-Bmu, Belorechensk, Russia). Lacquer KO-915 (GNIIKhTEOS, Moscow, Russia) was used as a protective material.

### 2.2. Methods

The vibrating concrete mix was made in a MIKS-B-140 concrete mixer. The loading order of the materials was as follows: water, SRPC, sand, and gravel. The mixing of the mixture in a concrete mixer was carried out until its homogeneous consistency was obtained. Next, the mixture was placed in metal molds in the form of cubes (2FK-50) and in the form of prisms (FB-50/200). Then the molds with the mixture were placed on a laboratory vibration platform (Figure 1a) and compacted for 50 s. After that, the mixture was aligned with the upper edges of the molds and placed before being removed from the molds for 1 day in a normal hardening chamber (air temperature 20 ± 2 °C, relative humidity 95 ± 5%). After being removed from the molds, the samples continued to harden under normal conditions for another 27 days.

The preparation of the concrete mixture using centrifugation and vibrocentrifugation technologies was carried out according to the following parameters: rotation speed—156 rad/s, molding time—12 min; vibration parameters: height of clamp projections—5 mm, projection length—20 mm, pitch between projections—30 mm. The appearance of the centrifuge is shown in Figure 1b. In general, the technology for manufacturing concrete elements of an annular section using centrifugation and vibrocentrifugation technologies included the following main technological operations: dosing of concrete mixture components, mixing of concrete mixture, loading of concrete mixture into a mold, centrifugation/vibrocentrifugation process (Figure 1b,c), sludge discharge, holding for 24 h in the mold, and removing the element of the annular section from the mold. The production and testing of samples in the laboratory were carried out in a room with an air temperature of 20 ± 2 °C and relative humidity of 60 ± 5%.

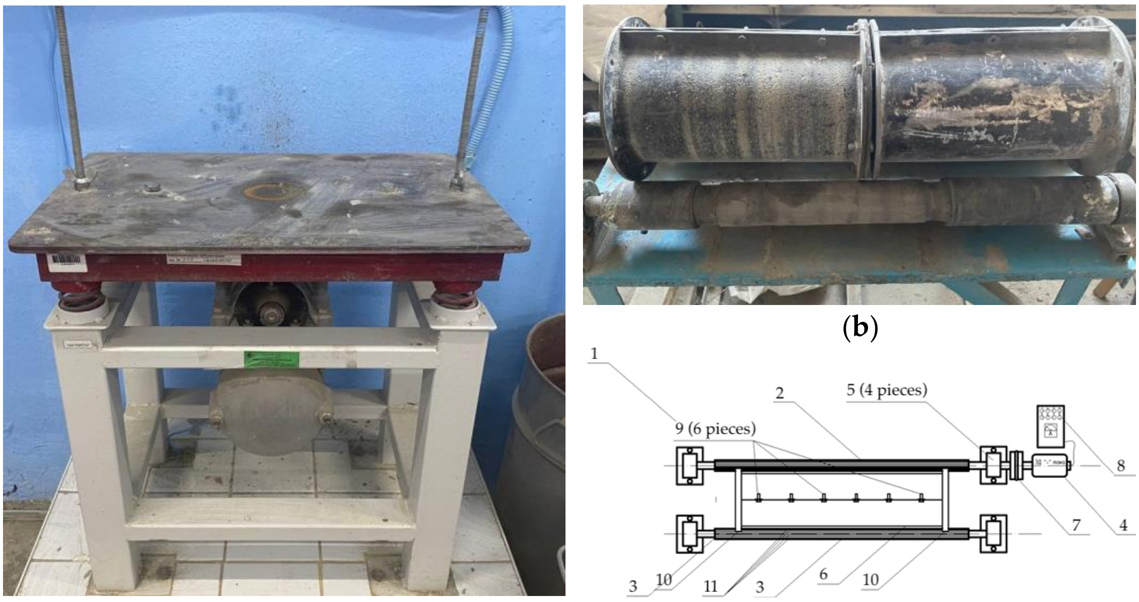


(**a**) (**c**)

**Figure 1.** Equipment for molding and compaction of samples: (**a**) laboratory vibrating platform for the manufacture of vibrated concrete samples; (**b**) photo and (**c**) drawing of a device for manufacturing samples of ring cross-section from centrifuged/vibrocentrifuged concrete.

The parameters of the vibrating platform (Figure 1a) are presented in Table 5.

**Table 5.** Technical characteristics of the laboratory vibration platform.

| Parameter | Value |
|---|---|
| Carrying capacity, up (kg) | 100 |
| The frequency of oscillations (oscillations in min) | 2900 ± 100 |
| Amplitude of oscillations (mm) | from 0.30 to 0.55 |
| Vibrator (type)<br>– Power (KW)<br>– Work voltage (V)<br>– Current frequency (Hz) | IV-99B<br>0.5<br>380<br>50 |
| Installation of forms on the table | Mechanical clamping bar |
| The overall dimensions of the vibration platform (mm)<br>– Length, no more<br>– Width, no more<br>– Height, no more | <br>580<br>400<br>580 |
| Weight, no more (kg) | 60 |

A device for the manufacture of products from centrifuged/vibrocentrifuged concrete containing a frame on which drive and support shafts, support rollers, shape, an electric motor with a coupling, and a thyristor control unit are mounted additionally contains steel ribs on the support and drive shafts (Figure 1c). The device consists of a frame 1, on which two shafts are mounted: drive 2 and support 3. The drive includes a multispeed electric motor 4 of a DC with a smooth adjustment of the thyristor control unit 8. A stop with supporting bearings 5 is supportive and can be adjusted depending on the diameter of form 6. The shafts of the drive 2 and the support 3 are made with the application of steel ribs 11, which provide high-frequency vibrations when moving the shape. The smoothness of the launch provides a clutch 7. The drive 2 and the support 3 shafts through the stops with the supporting bearings 5 are attached to the frame 1 using bolts 9 with a diameter of 12 mm. This device works as follows: on drive 2 and support shafts 3, a steel form of a given standard size 6 is installed; then there is a rotational movement from the electric motor 4 of DC with a thyristor control unit 2. Driving 2 and support 3 shafts through stops 5 are transmitted through the coupling 7 fixed to the frame 1 using bolts 9 with a diameter of 12 mm. Acceleration and smooth control of rotation speed are carried out due to the thyristor control unit 8, which allows one to change the speed of the engine of 4 DC. The rotation from the drive shaft 2 steel form 6 is transmitted due to friction forces. The steel form 6 has supports 10. The seal in steel form 6 occurs due to the action of the centrifugal sealing force on the components of the concrete mixture and high-frequency vibrational oscillation, which create steel ribs 11 on the drive 2 and the support of 3 shafts.

The study of the physical and mechanical characteristics of concrete during cyclic sulfate attack in the "dry–wet" states included the following steps:

- One cycle of sulfate attack lasted three days. Within 1 day, concrete samples were moistened in a 5% $Na_2SO_4$ solution (pH equal to 6 ± 0.1) (Figure 2), and then the samples were removed from the solution and kept for 2 days in an air environment at a temperature of 25 °C in a ventilated room.
- The test for cyclic sulfate attack was carried out for 180 days. After 5, 10, 15, 20, 25, 30, 35, 40, 45, 50, 55, and 60 cycles, the compressive strength was determined for cubic and prismatic samples, as was the weight loss of experimental samples.
- A total of 12 series of tests were carried out; for each series of tests, 3 cube samples 50 × 50 × 50 (mm) in size and 3 prism samples 50 × 50 × 200 (mm) in size were made. Thus, the total number of samples for cubes was 117, 9 controls (3 vibrated, 3 centrifuged, 3 vibrocentrifuged) and 108 for cyclic tests (36 vibrated, 36 centrifuged, 36 vibrocentrifuged). The total number of prism samples, similar to the number of cube samples, was 117.
- For the manufacture of vibrated concrete, a concrete mixture with a mass ratio of SRPC:sand:crushed stone:water = 1:1.3:2.6:0.52 was used [46], and for the manufacture of centrifuged and vibrocentrifuged concrete [47], a concrete mixture was used with a mass ratio of SRPC:sand:crushed stone:water = 1:1.44:2.48:0.41 (concrete mixing proportions in 1 $m^3$ are given in Table 6);

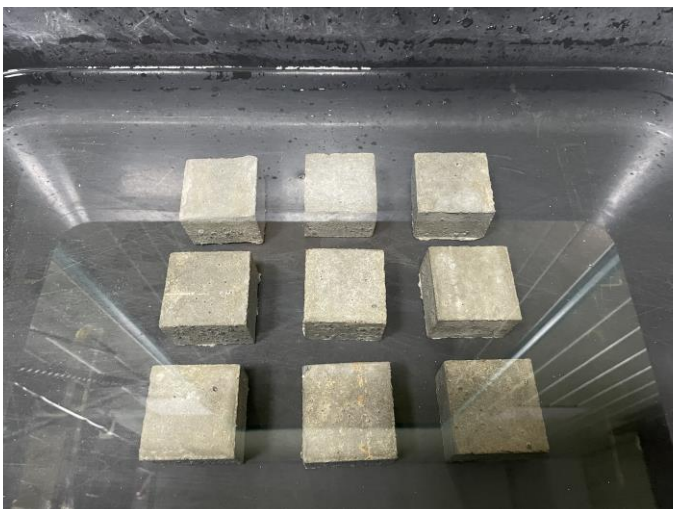

**Figure 2.** The process of moisturizing concrete samples in 5% $Na_2SO_4$ solution.

**Table 6.** Concrete mixing proportions in 1 $m^3$.

| Technology | SRPC ($kg/m^3$) | Water ($kg/m^3$) | Sand ($kg/m^3$) | Crushed Stone ($kg/m^3$) |
|---|---|---|---|---|
| Vibration | 395 | 205 | 514 | 1027 |
| Centrifugation and vibrocentrifugation | 405 | 166 | 583 | 1004 |

At the same time, the properties of the fresh state of vibrated, centrifuged, and vibrocentrifuged concrete almost did not differ from each other. The fresh state properties of vibrated, centrifuged, and vibrocentrifuged concretes are presented in Table 7.

**Table 7.** The fresh state properties of vibrated, centrifuged, and vibrocentrifuged concretes.

| Technology | Fresh Concrete Density ($kg/m^3$) | Workability (Grade) | Slump (cm) |
|---|---|---|---|
| Vibration | 2141 | P1 * | 3 |
| Centrifugation and vibrocentrifugation | 2158 | P1 | 2 |

* Fresh concrete workability grade according to GOST 7473 [48], corresponding to the slump of the cone 1–4 cm according to GOST 10181 [49].

Samples for determining the fresh state properties of concretes are shown in Figure 3.

– Production of vibrated, centrifuged, and vibrocentrifuged concretes, as well as sawing of variotropic concretes, was carried out according to the method presented in [34]. Photos of specimens for compression tests before failure and after are shown in Figure 4.

(a) (b)

**Figure 3.** Samples for determining the fresh state properties of (**a**) vibrated concrete and (**b**) variotropic concrete.

(a) (b)

**Figure 4.** Sample cubes, sawn from samples of an annular section: (**a**) at the top—before testing, at the bottom—after testing for sulfate attack; (**b**) after compression test.

Compressive testing of specimens was carried out according to GOST 10180-2012 [50] and GOST 28570-2019 [51] for cube strength and according to GOST 24452-80 [52] for prismatic strength.

The assessment of the concrete corrosion resistance in an acid solution (continuous sulfate attack), for samples made using the technologies of vibrating, centrifuging, and vibrocentrifuging, is based on the rate of change in the chemical composition of the $H_2SO_4$ acid solution and hardened cement paste in concrete immersed in a 5% concentration (pH equal to 4 ± 0.1) acid solution during diffusion transfer of an aggressive substance in concrete. The test was carried out at a temperature of 20 ± 3 °C as follows [53,54]:

- The samples were prepared in advance; namely, their side surfaces were covered with a protective coating. Then the prepared samples were placed in desiccators and filled with an acid solution. The distance between the working surfaces of the samples and neighboring samples, as well as to the surface of the mortar, was at least 2 cm. In total, 12 samples 50 × 50 × 50 mm in size were made for each type of concrete. The process of curing concrete samples in a sulfuric acid solution is shown in Figure 5.
- Before testing and periodically during testing, the acid concentration was determined by acid–base titration. Immediately before sampling, the acid solution was stirred; when the acid concentration decreased by 5 ± 0.1% compared to the initial acid solution, it was replaced with a new one.
- The total duration of testing samples was 180 days. In the first three weeks of testing, samples of the acid solution were taken and titrated daily; then, three times a week; and after 3 months of testing, twice a week.

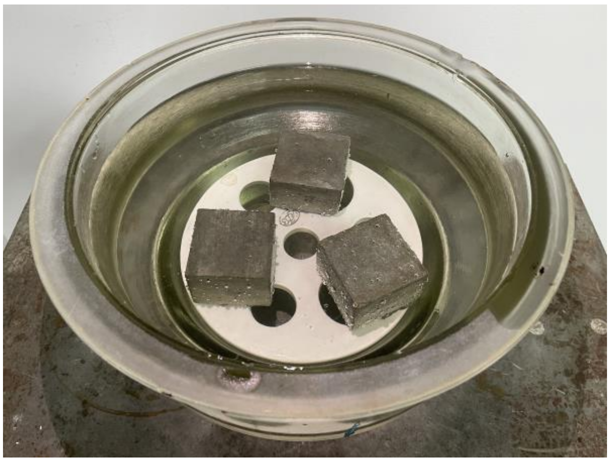

**Figure 5.** The process of curing concrete samples in a 5% solution of $H_2SO_4$.

When processing the test results, the amount of acid that entered into a chemical reaction with concrete was determined, and the amount of $Ca^{2+}$ ions that entered into a chemical reaction with acid was calculated. The amount of $Ca^{2+}$ ions that reacted with the acid was calculated as follows: The following indicators were set [53,54]:

- Periods between individual sampling $\tau_1, \tau_2, \ldots, \tau_i$ and the total time from the start of testing $\sum\tau$, days;

The area of the working surface of the samples that interacted with the acid S ($cm^2$);

The volume of the acid solution interacting with the concrete in each time period between individual tests Q ($cm^3$);

- The volume of a standard solution with a known concentration used for titration of the initial acid solution before testing $q_1$ ($cm^3$);
- The volume of a standard solution with a known concentration of a chemically active substance used for titration of the solution after interaction with concrete $q_2$ ($cm^3$);
- Volume of acid solution taken for titration $q_3$ ($cm^3$).

The amount of CaO that reacted with the acid was calculated for the period between sampling the solution of $P_{CaO}$ (g/cm$^2$). The total amount of CaO that reacted with the acid for the entire test period $\sum P_{CaO}$ (g/cm$^2$) was calculated.

The amount of hardened cement paste (calculated as CaO) chemically interacting with the acid solution during the period between two samplings was calculated using the following formula [53,54]:

$$P_{CaO} = \frac{(q_1 - q_2) M f_{eqv(CaO)} \times 0.05608 Q}{S q_3} \tag{1}$$

where $M$ is the molarity of the solution; $f_{eqv(CaO)}$ = 0.5; and 0.05608 is the molar mass of CaO, corresponding to 1 cm$^3$ of an acid solution with a concentration of 1 mol/dm$^3$.

The total amount of CaO that entered into the chemical reaction with the acid $\sum P_{CaO}$ was determined by summing $P_{CaO}$ for each test period [53,54]:

$$\sum P_{CaO} = P_{1CaO} + P_{2CaO} + \ldots + P_{nCaO} \tag{2}$$

The sulfate attack rate was calculated using the following formula [53,54]:

$$v = \frac{P_{1CaO}}{\tau} \tag{3}$$

The depth of destruction of concrete $D_\mathrm{d}$ was calculated using the following formula [53,54]:

$$D_d = \frac{\sum P_{CaO}}{C\beta} \tag{4}$$

where $C$ is the amount of cement in 1 cm$^3$ of the test sample, calculated from the actual composition of concrete (g/cm$^3$); $\beta$ is the CaO content in the cement, determined by the results of the chemical analysis of the cement before testing (%).

The general plan of experimental studies is shown in Figure 6.

The list of testing and technological equipment necessary for carrying out the declared experimental studies is presented in Table 8.

**Table 8.** Equipment and measuring instruments used in the study.

| Name of the Technological Operation | Equipment |
|---|---|
| Production of concrete mix | Concrete mixer MIKS-B-140 (Siberian Technologies, Chelyabinsk, Russia) |
| Forming and making concrete samples | Vibrated concrete—laboratory vibrating platform SMZh-539-220A (IMASH, Armavir, Russia), forms 2FK-50, FB50/200 (RNPO RusPribor, St. Petersburg, Russia); KNT-1 normal curing chamber (RNPO RusPribor, St. Petersburg, Russia), centrifuged and vibrocentrifuged concrete—laboratory centrifuge [55] |
| Sawing centrifuged and vibrocentrifuged concrete samples | Stone cutting machine Cedima CTS-175 (CEDIMA GmbH, Celle, Germany) |
| Carrying out cyclic tests | Scales VLTE-2100 (NPP Gosmetr, St. Petersburg, Russia), hydraulic press P-50 (RSTSIM, Moscow, Russia) |
| Conducting stationary tests to assess corrosion resistance | Analytical balance VL-324V (NPP Gosmetr, St. Petersburg, Russia), laboratory mercury thermometer TL-4 (ALFA-PRIBOR, Tula, Russia), pH-meter HANNA HI 98103 Checker 1 (Hanna Instruments, Nusfalau, Romania), measured laboratory glassware |
| Analysis of the structure of concrete samples after cyclic tests | Optical microscope MBS-10 (Measuring equipment, Moscow, Russia) |

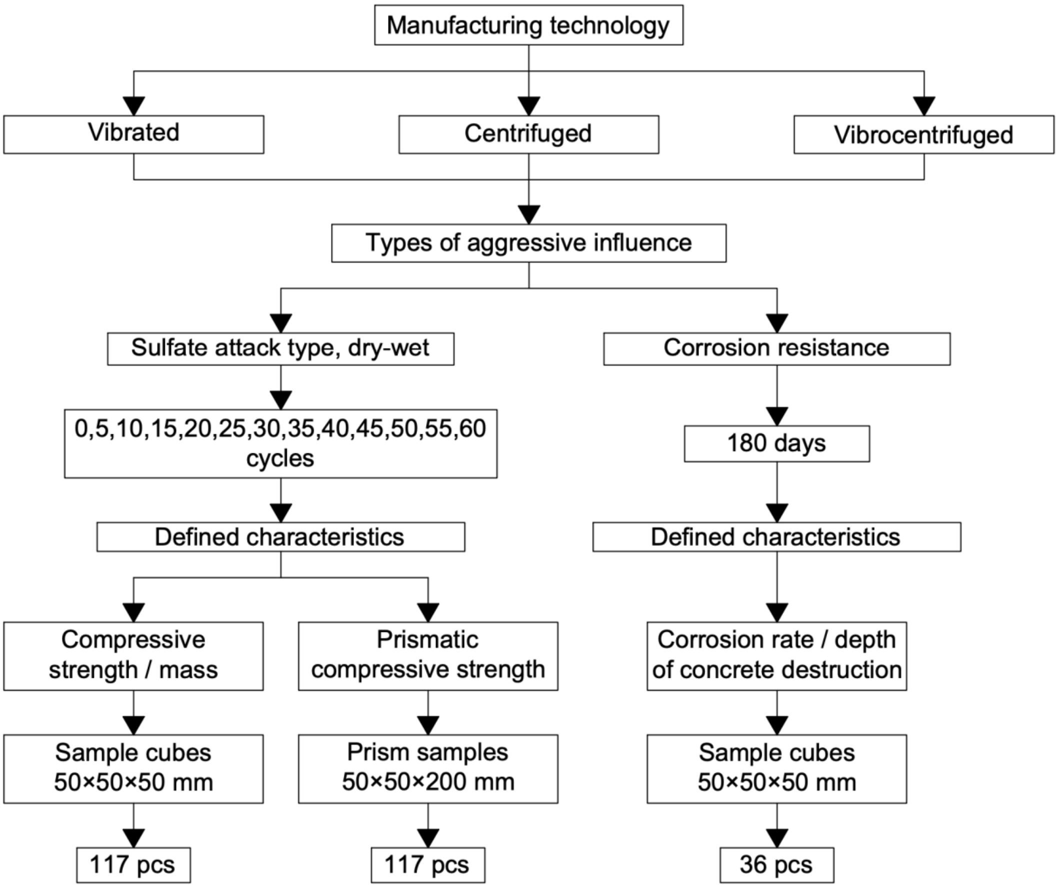


**Figure 6.** General plan of experimental studies.

## 3. Results and Discussion

### *3.1. Evaluation of Concrete Mass Loss during Cyclic Sulfate Attack*

Figure 7 shows the mass loss values of experimental samples depending on the number of sulfate attack cycles.

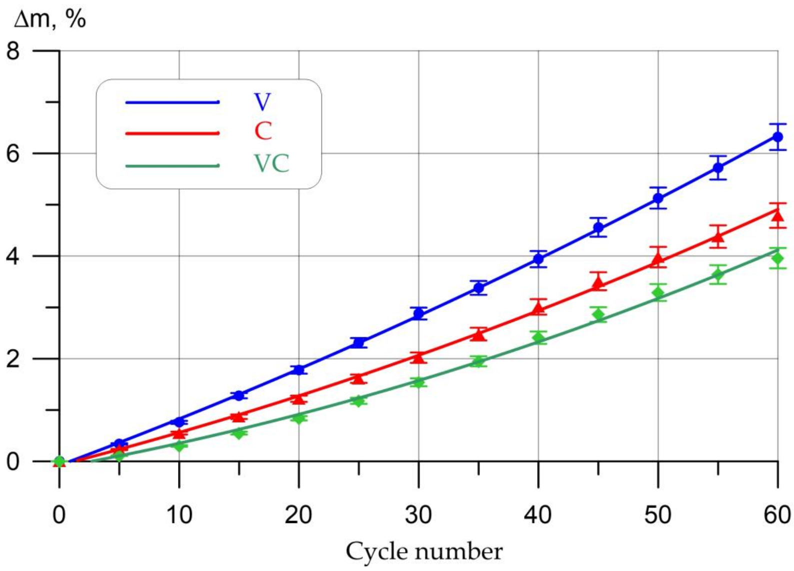


**Figure 7.** Concrete mass loss values depending on the number of sulfate attack cycles (V—vibrated, C—centrifuged, VC—vibrocentrifuged).

Figure 7 shows that with an increase in the number of sulfate attack cycles, the percentage of mass loss of concrete samples made using all three technologies also increases.

The dependences of the mass loss on cycle number $x$ shown in Figure 7 are well approximated by a polynomial of the second degree (5)–(7) with a high coefficient of determination $R^2$.

$$\Delta m_V = -0.0769 + 0.087x + 0.000335x^2, R^2 = 0.999 \quad (5)$$

$$\Delta m_C = -0.0735 + 0.0596x + 0.000389x^2, R^2 = 0.998 \quad (6)$$

$$\Delta m_{VC} = -0.1150 + 0.0421x + 0.000474x^2, R^2 = 0.996 \quad (7)$$

Figure 7 and Equations (5)–(7) show that the smallest percentage of weight loss after 60 cycles was recorded for vibrocentrifuged concretes and amounted to 3.96%; for centrifuged concretes, it is 4.79%, and for vibrated concretes, it is 6.32%. Thus, after 60 cycles of sulfate attack, the mass drop of vibrocentrifuged concrete is 17% less than that of centrifuged concrete, and 37% less than that of vibrated concrete.

### *3.2. Evaluation of the Strength Characteristics of Concrete under Cyclic Sulfate Attack*

The results of changes in the compressive strength of vibrated, centrifuged, and vibrocentrifuged concrete samples depending on the number of sulfate attack cycles are presented in Table 9 and Figure 8.

**Table 9.** Change in compressive strength of concrete samples depending on the number of sulfate attack cycles.

| Cycle Number | Manufacturing Technology | | |
|---|---|---|---|
| | Vibration | Centrifugation | Vibrocentrifugation |
| | Compressive Strength (MPa) | | |
| 0 | 43.7 | 47.3 | 50.8 |
| 5 | 43.5 | 47.2 | 50.7 |
| 10 | 43.1 | 46.9 | 50.5 |
| 15 | 42.5 | 46.5 | 50.2 |
| 20 | 41.7 | 46.0 | 49.7 |
| 25 | 41.0 | 45.4 | 49.3 |
| 30 | 40.3 | 44.7 | 48.7 |
| 35 | 39.5 | 44.1 | 48.1 |
| 40 | 38.8 | 43.6 | 47.7 |
| 45 | 38.4 | 43.0 | 47.2 |
| 50 | 37.7 | 42.5 | 46.8 |
| 55 | 37.2 | 42.1 | 46.4 |
| 60 | 36.5 | 41.7 | 46.0 |

An analysis of the trend in compressive strength change, shown in Figure 8, showed that the rate of compressive strength drop is the highest for vibrated concrete and the lowest for vibrocentrifuged concrete. Already after 15 cycles, there is a noticeable difference in the drop in strength of vibrated concrete in comparison with centrifuged and vibrocentrifuged concrete. So, in general, after 60 cycles of aggressive action, the loss of compressive strength was 16.4% for vibrated concrete, 11.8% for centrifuged concrete, and 9.5% for vibrocentrifuged concrete.

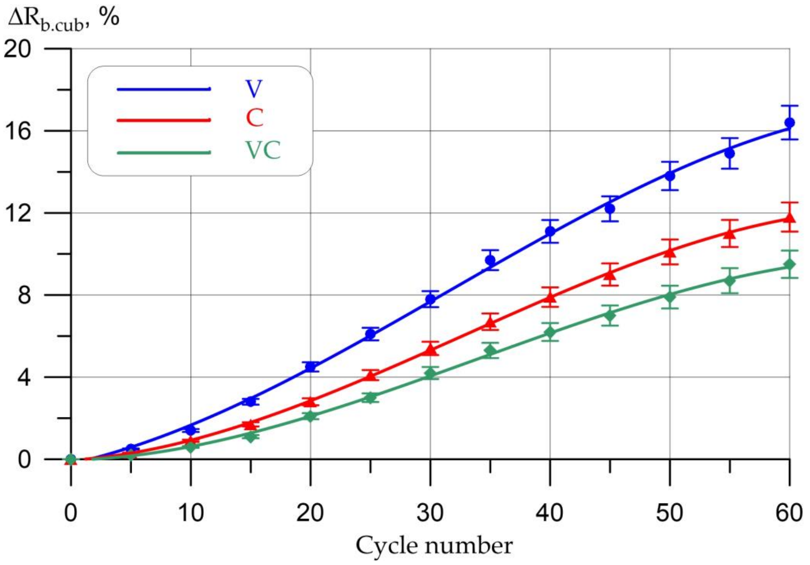


**Figure 8.** Dependence of the loss of compressive strength of concrete on the number of sulfate attack cycles (V—vibrated, C—centrifuged, VC—vibrocentrifuged).

The dependences of the loss of compressive strength on cycle number $x$ shown in Figure 8 are well approximated by a polynomial of the third degree (8)–(10) with a high coefficient of determination $R^2$.

$$\Delta R_{Vb.cub} = -0.2137 + 0.1290x + 0.00655x^2 - 6.946 \times 10^{-5}x^3, R^2 = 0.998 \quad (8)$$

$$\Delta R_{Cb.cub} = -0.0415 + 0.0353x + 0.006860x^2 - 6.969 \times 10^{-5}x^3, R^2 = 0.998 \quad (9)$$

$$\Delta R_{VCb.cub} = -0.04066 + 0.0134x + 0.00579x^2 - 5.687 \times 10^{-5}x^3, R^2 = 0.998 \quad (10)$$

The results of changes in the axial compressive strength (prism strength) of vibrated, centrifuged, and vibrocentrifuged concrete samples depending on the number of sulfate attack cycles are presented in Table 10 and Figure 9.

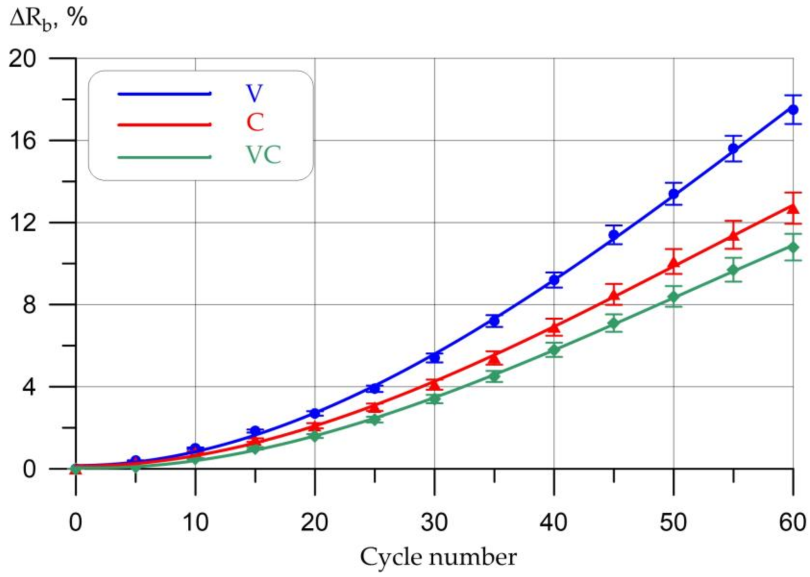


**Figure 9.** Dependence of the loss of prism compressive strength of concrete on the number of sulfate attack cycles (V—vibrated, C—centrifuged, VC—vibrocentrifuged).

**Table 10.** Change in prism compressive strength of concrete samples depending on the number of sulfate attack cycles.

| Cycle Number | Manufacturing Technology | | |
|---|---|---|---|
| | Vibration | Centrifugation | Vibrocentrifugation |
| | Compressive Strength (MPa) | | |
| 0 | 32.6 | 35.9 | 38.1 |
| 5 | 32.5 | 35.8 | 38.1 |
| 10 | 32.3 | 35.6 | 37.9 |
| 15 | 32.0 | 35.4 | 37.7 |
| 20 | 31.7 | 35.1 | 37.5 |
| 25 | 31.3 | 34.8 | 37.2 |
| 30 | 30.8 | 34.4 | 36.8 |
| 35 | 30.3 | 34.0 | 36.4 |
| 40 | 29.6 | 33.4 | 35.9 |
| 45 | 28.9 | 32.8 | 35.4 |
| 50 | 28.2 | 32.3 | 34.9 |
| 55 | 27.5 | 31.8 | 34.4 |
| 60 | 26.9 | 31.3 | 34.0 |

The dependences of prismatic compressive strength on cycle number $x$ are approximately similar to the trend in cubic compressive strength (Equations (11)–(13)).

$$\Delta R_{Vb} = 0.160 - 0.001176x + 0.007272x^2 - 3.980 \times 10^{-5}x^3, R^2 = 0.998 \quad (11)$$

$$\Delta R_{Cb} = 0.135 - 0.004086x + 0.005851x^2 - 3.753 \times 10^{-5}x^3, R^2 = 0.999 \quad (12)$$

$$\Delta R_{VCb} = 0.060 - 0.01674x + 0.005414x^2 - 3.543 \times 10^{-5}x^3, R^2 = 0.999 \quad (13)$$

Already after 20 cycles, the strength reduction rate of vibrated concrete increases sharply and is the highest among the three types of concrete under consideration. The minimum rate of strength drop was recorded for vibrocentrifuged concrete. The maximum drop in prism compressive strength after 60 cycles of sulfate attack was 17.5% for vibrated concrete, 12.7% for centrifuged concrete, and 10.8% for vibrocentrifuged concrete.

It should be noted that in the dependences obtained (5)–(13), the first term of the polynomials is close to zero (within the measurement error). This means that if the number of sulfate attacks $x$ is zero, then there is no loss of mass and strength.

### *3.3. Assessment of Structural Changes in Concrete after Cyclic Sulfate Attack*

Samples after cyclic tests with sulfate attack were examined using an optical microscope to compare the structure of concretes made using the three technologies under consideration—vibrating, centrifuging, and vibrocentrifuging. Photos of the structure of concrete samples are shown in Figures 10–12.

Figure 10 shows that the structure of vibrated concrete after 30 cycles (Figure 10a) and especially after 60 sulfate attack cycles (Figure 10b) has defects in the form of structure breaks, large pores, air channels, and cracks. Such defects are already much less pronounced, and they are not so noticeable in samples of centrifuged concrete (Figure 11). As for vibrocentrifuged concrete, its samples have minor structural defects in the initial stage of development (Figure 12). In concrete, under the action of aggressive waters containing sulfates, destruction manifests itself in the form of swelling and curvature of structural elements. In this case, not only does the removal of components from the volume of cement stone occur, but, on the contrary, as a result of chemical reactions between it and substances coming from the external environment, new compounds are formed, the volume of which exceeds the volume of the solid phase of the components of the hardened cement paste. An example of such corrosion is the formation of a "cement bacillus"—calcium hydrosulfoaluminate. Calcium hydrosulfoaluminates occupy a volume approximately 2.5 times larger than that of the original calcium aluminate. As a result, internal stresses appear, causing the appearance of cracks. The result of this type of corrosion is sometimes the formation of bubbles on the concrete surface—the phenomenon of local delamination. It consists in the fact that flat round fragments begin to bounce off the concrete [56].

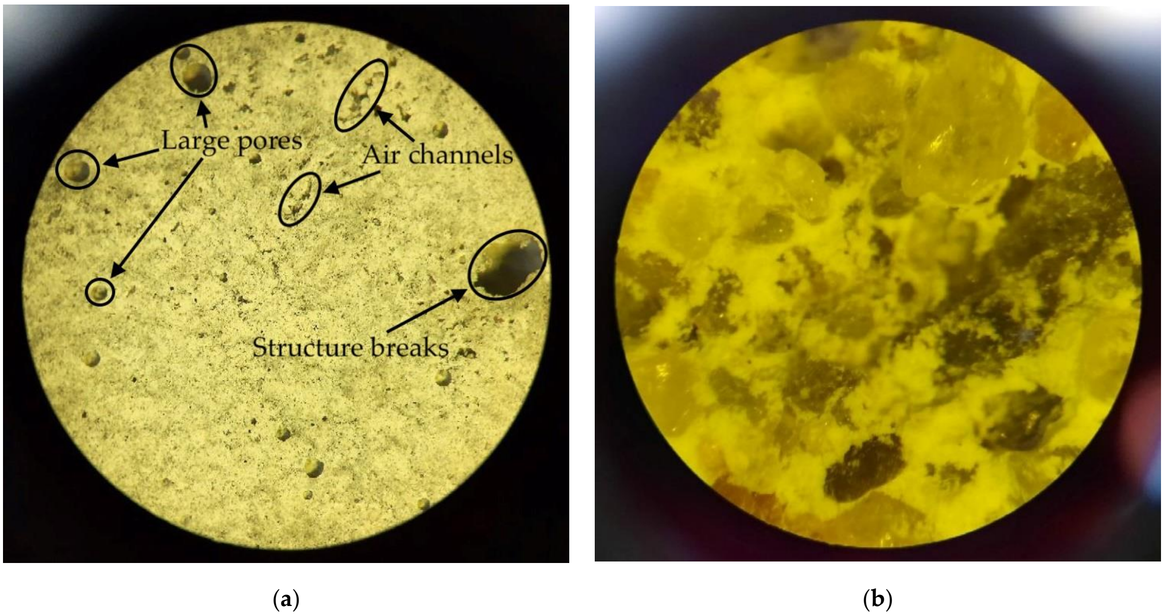


**Figure 10.** Samples of vibrated concrete after cyclic sulfate attack at 8× magnification: (**a**) after 30 cycles; (**b**) after 60 cycles.

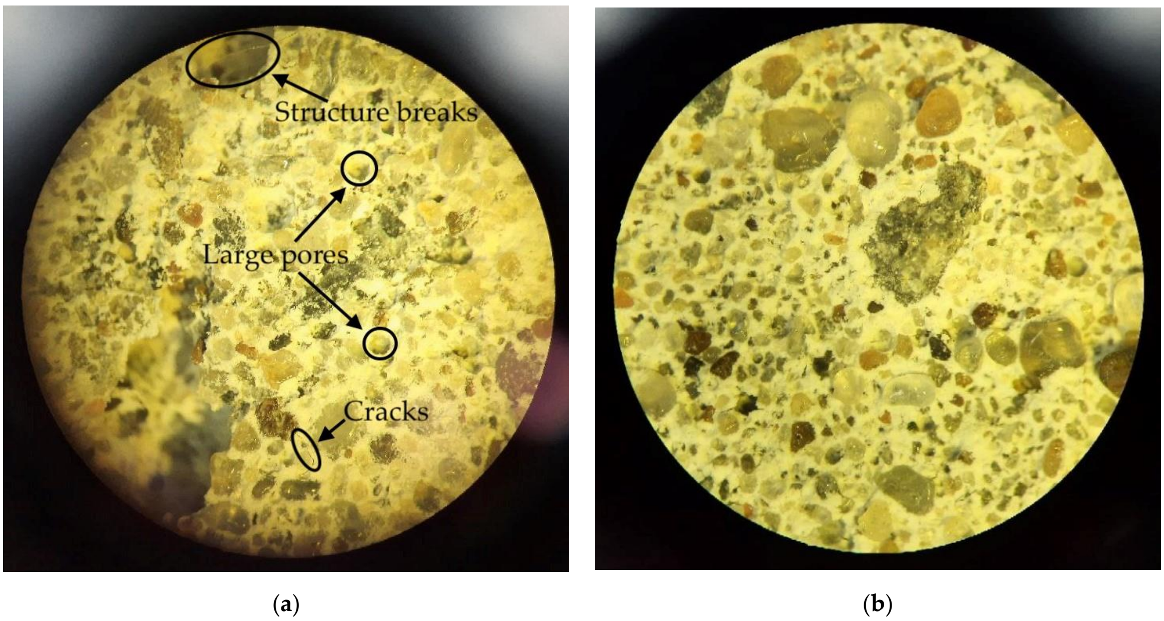


**Figure 11.** Centrifuged concrete samples after cyclic sulfate attack at 8× magnification: (**a**) after 30 cycles; (**b**) after 60 cycles.

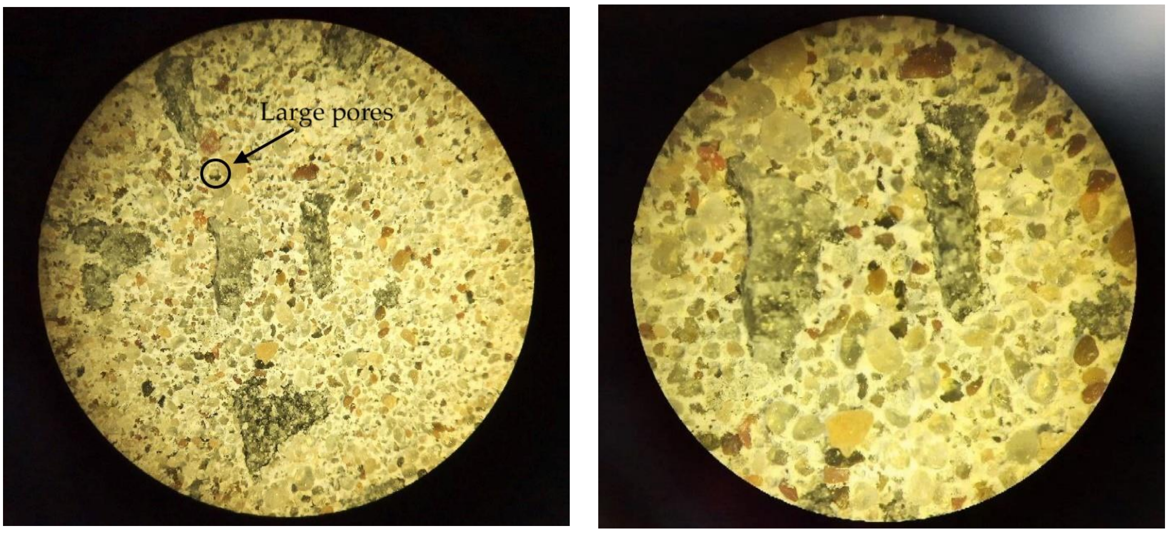


(**a**) (**b**)

**Figure 12.** Samples of vibrocentrifuged concrete after cyclic sulfate attack at 8× magnification: (**a**) after 30 cycles; (**b**) after 60 cycles.

In general, from the analysis of the structure of variotropic (centrifuged and vibrocentrifuged) concrete, it follows that the outer and middle layers of this type of concrete are the densest structure with fewer pores compared to the inner layer. The inner layer can be the main source of reduced concrete resistance. Structural pores in this layer are mainly represented by filtration channels, the number and size of which increase as they approach the inner cavity of the product. The hardened cement paste of this layer is characterized by a significant volume of capillary pores: approximately 25% of the total number of macropores in centrifuged concrete. Thus, by providing protection from the inner layer, it is possible to achieve high rates of sulfate attack [38,57–59].

### *3.4. Evaluation of the Resistance of Concrete to Continuous Sulfate Attack*

The results of assessing the resistance of vibrated, centrifuged, and vibrocentrifuged concrete to sulfate attack after holding for 180 days in a 5% sulfuric acid solution are presented in Table 11.

**Table 11.** Indicators of sulfate attack.

| **Sulfate Attack Index** | **Concrete Type** | | |
|---|---|---|---|
| | **Vibration** | **Centrifugation** | **Vibrocentrifugation** |
| Sulfateattackrate$\left(\frac{\text{mgCaO}}{\text{cm}^2\text{days}}\right)$ | 7.1 | 6.0 | 5.2 |
| Depth of destruction of concrete (mm) | 3.21 | 2.07 | 1.11 |

According to the results of experimental studies, concretes made using vibrocentrifugation technology have the best indicators of sulfate attack. The sulfate attack rate of vibrocentrifuged concrete turned out to be 13% less than that of centrifuged concrete and 27% less than that of vibrated concrete. The depth of destruction of vibrocentrifuged concrete is 46% less than that of centrifuged concrete and 65% less than that of vibrated concrete.

### *3.5. Discussion*

The essence of sulfate attack is that the hydroxide and calcium hydroaluminate contained in concrete enter into a chemical reaction with sulfate ions to form gypsum and calcium hydroaluminate. The reaction products are deposited on the walls of the pores and partially clog them. Further, if highly soluble alkalis are not formed in the reaction zone, the pH will gradually decrease with an increase in the acidity of the pore fluid, which in turn leads to the hydrolysis of first high-aluminate and gradually low-aluminate calcium hydrosilicates included in the framework of the concrete matrix. The gradual destruction of the concrete structure leads to the loss of its strength [60].

In general, the results obtained in this study are in good agreement with a number of other studies that also studied the effect of sulfate attack on the physical and mechanical properties of various types of concrete [2–6,12–14,16–21]. As the main positions for comparing the obtained results with the results of other authors, we can single out the loss of strength characteristics and mass. A trend similar to this study for a decrease in strength characteristics and a decrease in weight with an increase in the number of sulfate attack cycles is observed in [2,4,16]. But unlike [2], where the strength properties of concrete after 10–15 cycles of sulfate attack slightly increased, in the current study, the strength properties from the first cycle of sulfate attack do not exceed the control values, and only decrease with an increase in the number of cycles. With regard to the determination of the resistance of concrete in an acid solution, [8] can be considered similar in terms of the acid environment used. The sulfate attack mode chosen in this study coincided with the drying conditions but differed in the duration of the "dry–wet" cycles from [61].

So, the scientific novelty of the study can be considered the first created data system for three technologies, namely vibrating, centrifuging, and vibrocentrifuging of concrete, depending on sulfate attack. In view of the fact that all methods of protection against sulfate attack can be divided into two groups, namely the prescription and technological ones, we will evaluate the achievements of each of these methods separately. Laboratory experimental results have shown that vibrocentrifuged concrete has the highest degree of resistance to sulfate attack, and centrifuged concrete has a slightly lower resistance, while traditional vibrated non-variotropic concrete has the lowest resistance. Such differences and advantages of some technologies over others are due to differences in the structure of the concrete itself. The phenomenon of variotropy thus creates additional protection and the effect of protection from sulfate attack for concretes used in structures with increased responsibility. These conditions include a wide range of operating conditions. Thus, the stability of variotropic vibrocentrifuged concretes of reinforced concrete structures of critical facilities will be ensured only by a technological solution that occurs during the regrouping of centrifugation technology to vibrocentrifugation. This is a technologically simple way; however, the result of such an intervention in technology is very high, and therefore, the technological advantages of vibrocentrifuged concretes are proved, as in previous articles [34,41]. In addition, the high efficiency of vibrocentrifugation is confirmed in [35–40]. In general, vibrocentrifugation, being a developed stage of the centrifugation process, and its high effect are in good agreement with [42,43]. As for vibrated concrete, in this case, it is technologically difficult to achieve positive variotropy due to the peculiarities of compaction by vibration. Therefore, for vibrated structures, it is recommended to use the traditional method of increasing the resistance to sulfate attack through recipe methods. These can be specified dosages, compositions, or the use of special additives that will slightly increase the resistance to sulfate attack of vibrated concrete, if necessary. However, we repeat that, technologically, the greatest efficiency for operation in such conditions was shown by vibrocentrifuged concrete.

Let us explain the physical essence of this process. As we have already proved earlier [34,41], the structure of such concrete has a more perfect form, both at the level of microporosity and at the level of macroporosity. The porous structure of the outer layer, which is a protective shield for the entire structure, allows it to withstand corrosion phenomena and impacts and protects weaker inner layers, including those in which reinforcing elements are located. Thus, an additional emerging compacted layer, which is also present in centrifuged concrete, but is most pronounced in vibrocentrifuged concrete, creates structural and technological protection, and thus, the destructive mechanism of sulfate attack is slowed. Figure 13 shows a sample sawn from a concrete sample of an annular section, where one can visually observe the characteristic previously selected layers.

**Figure 13.** Concrete sample of variotropic structure.

Thus, we have technologically and experimentally proven the advantages of vibrocentrifuged concrete technology. This technology is proposed for implementation in structures operating in special conditions with an increased risk of sulfate attack in concrete and reinforced concrete.

If we talk about variotropic concretes made using centrifugation and vibrocentrifugation technologies, then the main means of increasing their corrosion resistance is to increase the average density of concrete. This can be achieved through the following recipe and technological solutions (Figure 14).

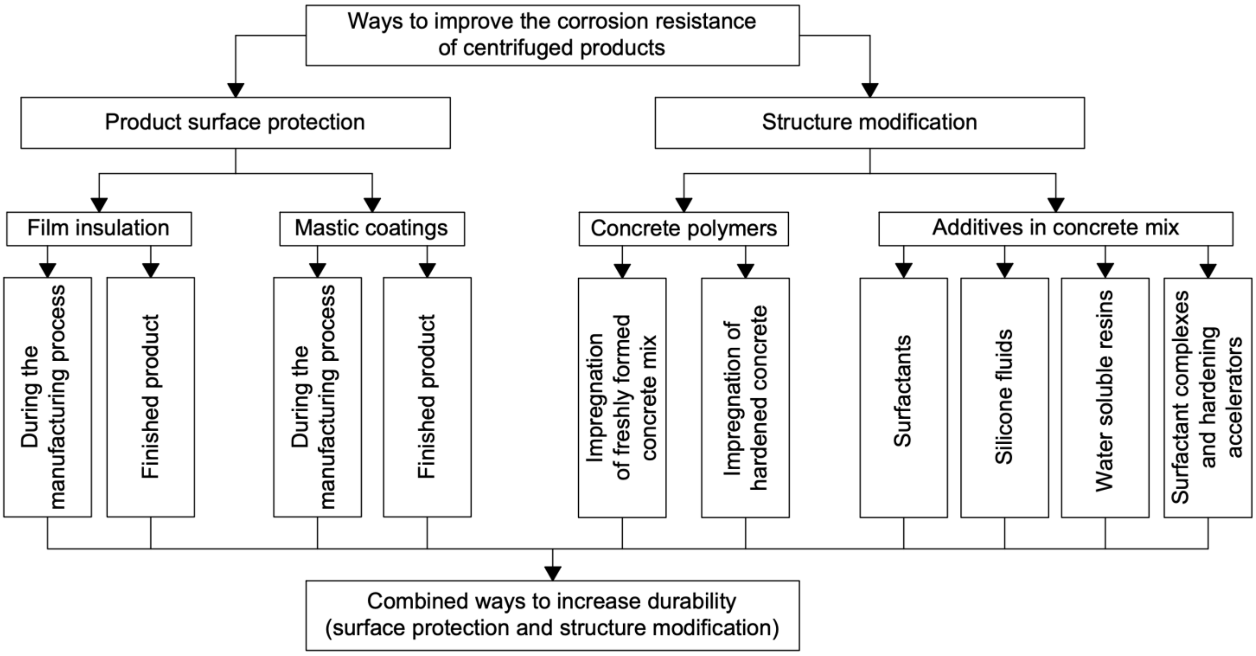


**Figure 14.** Ways to improve the resistance of variotropic concrete to corrosion.

Structure modification with the introduction of additives is an effective and widely used method for increasing corrosion resistance. The undoubted advantage of this method is the manufacturability and low cost of most additives. However, it should be borne in mind that the effect of additives in vibrated and centrifuged concrete may not be the same. The use of surfactants, organosilicon liquids, and water-soluble resins does not exclude the formation of directional porosity—migratory pores and channels—in the inner layers of centrifuged products, which will not provide them with the required increase in the resistance of concrete and the service life of products and structures made of it. This necessitates a special assessment of the effectiveness of traditional additives under conditions of aggressive action on variotropic concrete. The greatest technical effect can be obtained by impregnating the hardened inner layer of concrete with a monomer followed by its polymerization. In centrifuged and vibrocentrifuged concrete, directional porosity is eliminated, which is its main drawback [59].

The obtained results and the developed dependencies can be used as the foundation for new normative and technical documents and updated standards. In general, this approach is aimed at optimizing construction and technical processes, saving material, economic, and labor resources in terms of a more accurate assessment of the durability and life cycle of reinforced concrete structures that have hidden reserves due to the phenomenon of variotropy.

## 4. Conclusions

Based on the results of the resistance of traditional vibrated, centrifuged and vibrocentrifuged concrete to sulfate attack and their analysis, comparison, and discussion, the following conclusions were formulated:

(1) As a result of 60 sulfate attack cycles, the maximum mass loss was 6.32% for vibrated concrete, 4.79% for centrifuged concrete, and 3.96% for vibrocentrifuged concrete. The mass loss of vibrocentrifuged concrete is the smallest in comparison with centrifuged (17% less) and vibrated concrete (37% less).

(2) The compressive strength after 60 sulfate attack cycles decreased by 16.4% for vibrated concrete, 11.8% for centrifuged concrete, and 9.5% for vibrocentrifuged concrete. The loss of prismatic compressive strength for the same types of concrete was 17.5%, 12.7%, and 10.8%, respectively. The loss of cube and prism strength of vibrocentrifuged concrete is the smallest in comparison with centrifuged (20% and 18% less, respectively) and vibrated concrete (42% and 38% less, respectively).

(3) Comparative analysis of the structure of concrete samples after 60 cycles of sulfate attack revealed less defectiveness of the structure of vibrocentrifuged concrete in comparison with samples of centrifuged and vibrated concrete.

(4) Based on the results of assessing the sulfate attack resistance of concrete aged continuously for 180 days in a 5% sulfuric acid solution, the lowest sulfate attack rate and depth of destruction were recorded for vibrocentrifuged concrete. The sulfate attack rate of vibrocentrifuged concrete turned out to be 13% less than that of centrifuged concrete and 27% less than that of vibrated concrete. The depth of destruction of vibrocentrifuged concrete is 46% less than that of centrifuged concrete and 65% less than that of vibrated concrete.

Vibrocentrifugation technology is proposed for implementation in structures operated in special conditions with an increased risk of sulfate attack in concrete. Prospects for further research are seen in the direction of studying the effect of other types of attack and the formulation methods analyzed in this work on the resistance of variotropic concretes.

**Author Contributions:** Conceptualization, S.A.S., E.M.S., A.N.B. and D.E.; methodology, S.A.S., E.M.S. and A.C.; software, S.A.S., E.M.S., A.N.B. and A.C.; validation, D.E., S.A.S., E.M.S. and A.N.B.; formal analysis, A.C., S.A.S. and E.M.S.; investigation, D.E., L.R.M., S.A.S., E.M.S., A.N.B. and B.M.; resources, B.M.; data curation, S.A.S., E.M.S. and A.C.; writing—original draft preparation, S.A.S., E.M.S. and A.N.B.; writing—review and editing, S.A.S., E.M.S. and A.N.B.; visualization, S.A.S., E.M.S. and A.N.B.; supervision, L.R.M. and B.M.; project administration, L.R.M. and B.M.; funding acquisition, A.N.B. and B.M. All authors have read and agreed to the published version of the manuscript.

**Funding:** This research received no external funding.

**Institutional Review Board Statement:** Not applicable.

**Informed Consent Statement:** Not applicable.

**Data Availability Statement:** The study did not report any data.

**Acknowledgments:** The authors would like to acknowledge the administration of Don State Technical University for their resources and financial support.

**Conflicts of Interest:** The authors declare no conflict of interest.

## References

1. Fuhaid, A.; Niaz, A. Carbonation and Corrosion Problems in Reinforced Concrete Structures. *Buildings* **2022**, *12*, 586. [CrossRef]
2. Liu, J.; Li, A.; Yang, Y.; Wang, X.; Yang, F. Dry–Wet Cyclic Sulfate Attack Mechanism of High-Volume Fly Ash Self-Compacting Concrete. *Sustainability* **2022**, *14*, 3052. [CrossRef]
3. Terzijski, I.; Kocáb, D.; Štěpánek, P.; Strnad, J.; Girgle, F.; Šimůnek, P. Development of Variants of High-Performance Self-Compacting Concrete with Improved Resistance to the Attack of Sulfates. *Appl. Sci.* **2021**, *11*, 5945. [CrossRef]
4. Najjara, M.; Nehdi, M.; Soliman, A.; Azabi, T. Damage mechanisms of two-stage concrete exposed to chemical and physical sulfate attack. *Constr. Build. Mater.* **2017**, *137*, 141–152. [CrossRef]
5. Cheng, Y.; Dong, Y.; Diao, J.; Zhang, G.; Chen, C.; Wu, D. MSWI Bottom Ash Application to Resist Sulfate Attack on Concrete. *Appl. Sci.* **2019**, *9*, 5091. [CrossRef]
6. Maraveas, C. Durability Issues and Corrosion of Structural Materials and Systems in Farm Environment. *Appl. Sci.* **2020**, *10*, 990. [CrossRef]
7. Liang, X.; Qi, W.; Fang, Z.; Zhang, S.; Fan, Y.; Shah, S. Study on the Relationship between Chloride Ion Penetration and Resistivity of NAC-Cement Concrete. *Buildings* **2022**, *12*, 2044. [CrossRef]
8. Cheng, L.; Shi, L.; Yi, L.; Zhao, W. Study on Mechanical Properties and Constitutive Relationship of Concrete Corroded by Hydrochloric Acid under Cyclic Load. *Sustainability* **2022**, *14*, 4692. [CrossRef]
9. Cai, J.; Ran, Q.; Ma, Q.; Zhang, H.; Liu, K.; Zhou, Y.; Mu, S. Influence of a Nano-Hydrophobic Admixture on Concrete Durability and Steel Corrosion. *Materials* **2022**, *15*, 6842. [CrossRef]
10. Luo, Q.; Huang, J. Mechanisms and Critical Technologies of Transport Inhibitor Agent (TIA) throughout C-S-H Nano-Channels. *Materials* **2022**, *15*, 515. [CrossRef]
11. Zhao, C.; Jia, X.; Yi, Z.; Li, H.; Peng, Y. Mechanical Performance of Single-Graded Copolymer-Modified Pervious Concrete in a Corrosive Environment. *Materials* **2022**, *14*, 7304. [CrossRef] [PubMed]
12. Mostofinejad, D.; Nosouhian, F.; Nazari-Monfared, H. Influence of magnesium sulphate concentration on durability of concrete containing micro-silica, slag and limestone powder using durability index. *Constr. Build. Mater.* **2016**, *117*, 107–120. [CrossRef]
13. Lin, R.-S.; Wang, X.-Y.; Yi-Han. Effects of cement types and addition of quartz and limestone on the normal and carbonation curing of cement paste. *Constr. Build. Mater.* **2021**, *305*, 124799. [CrossRef]
14. Aperador, W.; Bautista-Ruiz, J.; Sánchez-Molina, J. Effect of Immersion Time in Chloride Solution on the Properties of Structural Rebar Embedded in Alkali-Activated Slag Concrete. *Metals* **2022**, *12*, 1952. [CrossRef]
15. Jiang, T.; Jin, Y. Influence of Magnesium Oxide on Carbonation of Cement Paste Containing Limestone and Metakaolin. *Sustainability* **2022**, *14*, 5627. [CrossRef]
16. Yang, B.; Ji, R.; Lan, Q.; Yang, J.; Xu, J. Sulfate Freeze–Thaw Resistance of Magnesium Potassium Phosphate Cement Mortar. *Materials* **2022**, *15*, 3342. [CrossRef] [PubMed]
17. Tassos, C.; Sideris, K.; Chatzopoulos, A.; Tzanis, E.; Katsiotis, M. Influence of the Type of Cement on the Durability of Concrete Structures Exposed to Various Carbonation Environments in Greece: A Contribution to the Sustainability of Structures. *Constr. Mater.* **2022**, *3*, 2. [CrossRef]
18. Wei, J.; Wang, Z.; Sun, W.; Yang, R. Durability Performance and Corrosion Mechanism of New Basalt Fiber Concrete under Organic Water Environment. *Materials* **2022**, *16*, 452. [CrossRef]
19. Wang, Z.-S.; Li, Y.-K.; Lu, J.-L.; Tian, J.-B.; Zhao, K. Research on Corrosion Characteristics and Performance Degradation of Basalt Fiber Concrete under Sodium Magnesium Sulfate Corrosion Environment. *J. Coast. Res.* **2020**, *111*, 56–62. [CrossRef]
20. Li, Y.; Chai, J.; Wang, R.; Zhou, Y.; Tong, X. A Review of the Durability-Related Features of Waste Tyre Rubber as a Partial Substitute for Natural Aggregate in Concrete. *Buildings* **2022**, *12*, 1975. [CrossRef]
21. Idrees, M.; Akbar, A.; Saeed, F.; Saleem, H.; Hussian, T.; Vatin, N. Improvement in Durability and Mechanical Performance of Concrete Exposed to Aggressive Environments by Using Polymer. *Materials* **2022**, *15*, 3751. [CrossRef]
22. Zhao, G.; Guo, M.; Li, S.; Weng, X.; Ding, S.; Han, F.; Wang, H. Influence of Ca+ on Early Degradation of Cast-In-Situ Mortar Induced by Sulfate-Magnesium Multiple Combined Attack. *Materials* **2022**, *15*, 5752. [CrossRef] [PubMed]
23. Ji, R.-J.; Li, T.; Yang, J.-M.; Xu, J. Sulfate Freeze–Thaw Resistance of Magnesium Potassium Phosphate Cement Mortar according to Hydration Age. *Materials* **2022**, *15*, 4192. [CrossRef] [PubMed]
24. Zhang, F.; Wei, F.; Wu, X.; Hu, Z.; Li, X.; Gao, L. Study on Concrete Deterioration and Chloride Ion Diffusion Mechanism by Different Aqueous NaCl-MgSO4 Concentrations. *Buildings* **2022**, *12*, 1843. [CrossRef]
25. Han, T.; Wang, X.; Li, D.; Li, D.; Han, N.; Xing, F. Damage and degradation mechanism for single intermittent cracked mortar specimens under a combination of chemical solutions and dry-wet cycles. *Constr. Build. Mater.* **2019**, *213*, 567–581. [CrossRef]
26. Zhang, T.; Wen, Q.; Gao, L.; Xu, Q.; Tang, J. Analytical Hysteretic Behavior of Square Concrete-Filled Steel Tube Pier Columns under Alternate Sulfate Corrosion and Freeze-Thaw Cycles. *Materials* **2022**, *15*, 3099. [CrossRef] [PubMed]
27. Refani, A.; Nagao, T. Corrosion Effects on the Mechanical Properties of Spun Pile Materials. *Appl. Sci.* **2022**, *13*, 1507. [CrossRef]

28. Chen, H.-J.; Chen, Y.-C.; Tang, C.-W.; Lin, X.-F. The Corrosion Resistance of Reinforced Lightweight Aggregate Concrete in Strong Brine Environments. *Materials* **2022**, *15*, 7943. [CrossRef]
29. Caballero, D.; Beltrán-Cobos, R.; Tavares, F.; Cruz-Yusta, M.; Granados, L.; Sánchez-Moreno, M.; Pavlovic, I. The Inhibitive Effect of Sebacate-Modified LDH on Concrete Steel Reinforcement Corrosion. *Chemengineering* **2022**, *6*, 72. [CrossRef]
30. Guo, Q.; Li, X.; Lin, N.; Liu, J. Influence of Rust Inhibitors on the Microstructure of a Steel Passive Film in Chloride Concrete. *Coatings* **2022**, *12*, 692. [CrossRef]
31. Uvida, M.; Almeida, A.; Pulcinelli, S.; Santilli, C.; Hammer, P. Structural Properties of Epoxy–Silica Barrier Coatings for Corrosion Protection of Reinforcing Steel. *Polymers* **2022**, *14*, 3474. [CrossRef] [PubMed]
32. De Domenico, D.; Messina, D.; Recupero, A. Seismic vulnerability assessment of reinforced concrete bridge piers with corroded bars. *Struct. Concr.* **2023**, *24*, 56–83. [CrossRef]
33. Guo, H.; Dong, Y.; Bastidas-Arteaga, E.; Gu, X.-L. Probabilistic failure analysis, performance assessment, and sensitivity analysis of corroded reinforced concrete structures. *Eng. Fail. Anal.* **2021**, *124*, 105328. [CrossRef]
34. Beskopylny, A.N.; Stel'makh, S.A.; Shcherban', E.M.; Mailyan, L.R.; Meskhi, B.; Chernil'nik, A.; El'shaeva, D.; Pogrebnyak, A. Influence of Variotropy on the Change in Concrete Strength under the Impact of Wet–Dry Cycles. *Appl. Sci.* **2023**, *13*, 1745. [CrossRef]
35. Mailyan, L.R.; Stel'makh, S.A.; Shcherban', E.M.; Khalyushev, A.K.; Smolyanichenko, A.S.; Sysoev, A.K.; Parinov, I.A.; Cherpakov, A.V. Investigation of Integral and Differential Characteristics of Variatropic Structure Heavy Concretes by Ultrasonic Methods. *Appl. Sci.* **2021**, *11*, 3591. [CrossRef]
36. Stel'makh, S.A.; Shcherban', E.M.; Beskopylny, A.N.; Mailyan, L.R.; Meskhi, B.; Butko, D.; Smolyanichenko, A.S. Influence of Composition and Technological Factors on Variatropic Efficiency and Constructive Quality Coefficients of Lightweight Vibro-Centrifuged Concrete with Alkalized Mixing Water. *Appl. Sci.* **2021**, *11*, 9293. [CrossRef]
37. Shcherban', E.M.; Stel'makh, S.A.; Beskopylny, A.; Mailyan, L.R.; Meskhi, B. Influence of Mechanochemical Activation of Concrete Components on the Properties of Vibro-Centrifugated Heavy Concrete. *Appl. Sci.* **2021**, *11*, 10647. [CrossRef]
38. Beskopylny, A.N.; Stel'makh, S.A.; Shcherban', E.M.; Mailyan, L.R.; Meskhi, B.; Beskopylny, N.; El'shaeva, D.; Kotenko, M. The Investigation of Compacting Cement Systems for Studying the Fundamental Process of Cement Gel Formation. *Gels* **2022**, *8*, 530. [CrossRef]
39. Beskopylny, A.N.; Meskhi, B.; Stel'makh, S.A.; Shcherban', E.M.; Mailyan, L.R.; Veremeenko, A.; Akopyan, V.; Shilov, A.V.; Chernil'nik, A.; Beskopylny, N. Numerical Simulation of the Bearing Capacity of Variotropic Short Concrete Beams Reinforced with Polymer Composite Reinforcing Bars. *Polymers* **2022**, *14*, 3051. [CrossRef]
40. Beskopylny, A.N.; Stel'makh, S.A.; Shcherban', E.M.; Mailyan, L.R.; Meskhi, B.; Beskopylny, N.; El'shaeva, D. Influence of the Chemical Activation of Aggregates on the Properties of Lightweight Vibro-Centrifuged Fiber-Reinforced Concrete. *J. Compos. Sci.* **2022**, *6*, 273. [CrossRef]
41. Beskopylny, A.N.; Shcherban, E.M.; Stel'makh, S.A.; Mailyan, L.R.; Meskhi, B.; Chernil'nik, A.; El'shaeva, D. Influence of Variatropy on the Evaluation of Strength Properties and Structure Formation of Concrete under Freeze-Thaw Cycles. *J. Compos. Sci.* **2023**, *7*, 58. [CrossRef]
42. Kliukas, R.; Lukoševičienė, O.; Jaras, A.; Jonaitis, B. The Mechanical Properties of Centrifuged Concrete in Reinforced Concrete Structures. *Appl. Sci.* **2020**, *10*, 3570. [CrossRef]
43. Feng, B.; Zhu, Y.-H.; Xie, F.; Chen, J.; Liu, C.-B. Experimental Investigation and Design of Hollow Section, Centrifugal Concrete-Filled GFRP Tube Columns. *Buildings* **2021**, *11*, 598. [CrossRef]
44. GOST 8269.0-97 Mauntainous Rock Road-Metal and Gravel, Industrial Waste Products for Construction Works Methods of Physical and Mechanical Tests. Available online: https://docs.cntd.ru/document/1200003066 (accessed on 10 February 2023).
45. GOST 8735-88 Sand for Construction Work. Testing Methods. Available online: https://docs.cntd.ru/document/1200003348 (accessed on 10 February 2023).
46. GOST 27006-2019 Concretes. Rules for Mix Proposing. Available online: https://docs.cntd.ru/document/1200165762 (accessed on 2 March 2023).
47. VSN 1-90 Fabrication Requirements for Centrifugal-Cast Support Pillars for Contact Lines, Communications Lines, and Lock-Out Systems. Available online: https://meganorm.ru/Index2/1/4294851/4294851029.htm (accessed on 2 March 2023).
48. GOST 7473-2010 Fresh Concrete. Specifications. Available online: https://docs.cntd.ru/document/1200085075 (accessed on 13 March 2023).
49. GOST 10181-2014 Concrete Mixtures. Methods of Testing. Available online: https://docs.cntd.ru/document/1200115733 (accessed on 13 March 2023).
50. GOST 10180-2012 Concretes. Methods for Strength Determination Using Reference Specimens. Available online: http://docs.cntd.ru/document/1200100908 (accessed on 10 February 2023).
51. GOST 28570-2019 Concretes. Methods of Strength Determination on Cores Selected from Structures. Available online: https://docs.cntd.ru/document/1200164023 (accessed on 27 February 2023).
52. GOST 24452-80 Concretes. Methods of prismatic, Compressive Strength, Modulus of Elasticity and Poisson's Ratio Determination. Available online: https://docs.cntd.ru/document/9056198 (accessed on 10 February 2023).
53. GOST R 52804-2007 Protection against Corrosion of Concrete and Reinforced Concrete Constructions. Test Methods. Available online: https://docs.cntd.ru/document/1200061316 (accessed on 10 February 2023).

54. GOST 31383-2007 Protection against Corrosion of Concrete and Reinforced Concrete Constructions. Test Methods. Available online: https://docs.cntd.ru/document/1200076445 (accessed on 27 February 2023).
55. Stel'makh, S.A.; Shcherban', E.M.; Kholodnyak, M.G.; Nasevich, A.S.; Yanovskaya, A.V. Device for the Manufacture of Products from Vibrocentrifuged Concrete. Russian. Federation Patent 197610, 29 January 2020. Available online: https://patentimages.storage.googleapis.com/99/a7/e4/7331df00d4bdba/RU197610U1.pdf (accessed on 10 February 2023).
56. Recommendations for Corrosion Protection of Concrete and Reinforced Concrete Building Structures of a Water Treatment Plant. Available online: https://docs.cntd.ru/document/1200035522. (accessed on 27 February 2023).
57. Akhverdov, I.N. *Reinforced Concrete Pressure Centrifuged Pipes*; Stroyizdat: Stroyizdat, Moscow, 1967; 164p, Available online: https://search.rsl.ru/ru/record/01005953134 (accessed on 14 February 2023).
58. Akhverdov, I.N. *Fundamentals of Concrete Physics*; Stroyizdat: Stroyizdat, Moscow, 1981; 464p, Available online: https://search.rsl.ru/ru/record/01001052337 (accessed on 14 February 2023).
59. Podurovskiy, N.I.; Zheltukhina, L.I. Development of ways to improve the durability and efficiency of products for energy construction. *Sci. Tech. Rep.* **1977**, *77005974*, 52–65.
60. Voloshina, N.A. Mechanism of sulfate corrosion and ways to protect concrete. *Bull. Sib. Fed. Univ. Comms* **2007**, *17*, 229–231.
61. Guo, J.-J.; Liu, P.-Q.; Wu, C.-L.; Wang, K. Effect of Dry–Wet Cycle Periods on Properties of Concrete under Sulfate Attack. *Appl. Sci.* **2021**, *11*, 888. [CrossRef]